EXHIBIT I

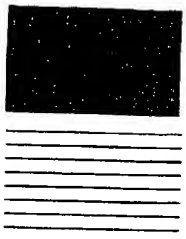

OPTICS

SECOND EDITION

EUGENE HECHT
Adelphi University

With Contributions by Alfred Zajac

ADDISON-WESLEY PUBLISHING COMPANY
Reading, Massachusetts • Menlo Park, California • Don Mills, Ontario
Wokingham, England • Amsterdam • Sydney • Singapore
Tokyo • Madrid • Bogotá • Santiago • San Juan

Sponsoring editor: Bruce Spatz
Production supervisors: Margaret Pinette and Lorraine Ferrier
Text designer: Joyce Weston
Illustrators: Oxford Illustrators
Art consultant: Loretta Bailey
Manufacturing supervisor: Ann DeLacey

Library of Congress Cataloging-in-Publication Data

Hecht, Eugene.
Optics.

Bibliography: p.
Includes indexes.
1. Optics. I. Zajac, Alfred. II. Title.
QC355.2.H42 1987 535 86-14067
ISBN 0-201-11609-X

Reprinted with corrections May, 1990.

10 11 12 13 14 15 VB 96959493

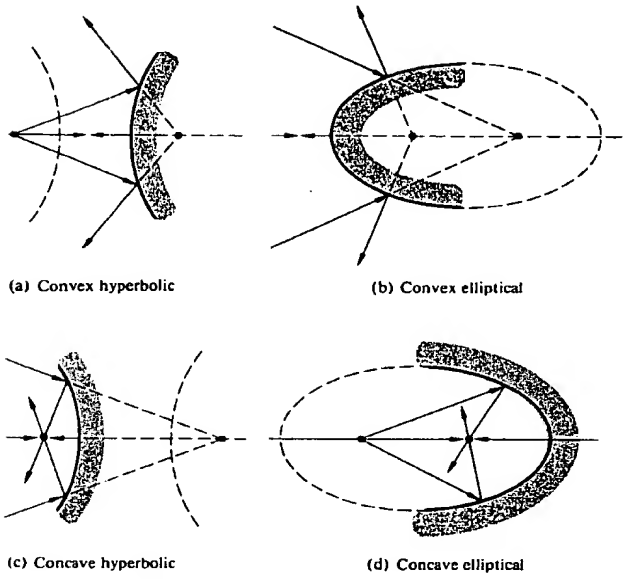

Figure 5.46 Hyperbolic and elliptical mirrors.

It should be noted that all these devices are readily available commercially. In fact, one can purchase *off-axis elements*, in addition to the more common centered systems. Thus, in Fig. 5.47 the focused beam can be further processed without obstructing the mirror.

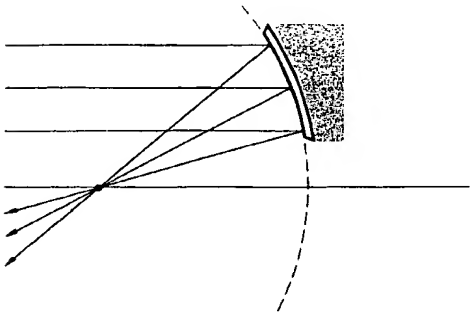

Figure 5.47 An off-axis parabolic mirror element.

Incidentally, this geometry also obtains in large microwave horn antennas, which have a significant role in modern communications.

5.4.3 Spherical Mirrors

We are again reminded of the fact that precise aspheric surfaces are considerably more difficult to fabricate than are spherical ones. The high costs are commensurate with the increased time and meticulous effort required. Motivated by these practical considerations, we once more turn to the spherical configuration to determine the circumstances under which it might perform adequately.

i) The Paraxial Region

The well-known equation for the circular cross-section of a sphere [Fig. 5.48(a)] is

$$y^2 + (x - R)^2 = R^2, \tag{5.43}$$

where the center C is shifted from the origin O by one radius R. After writing this as

$$y^2 - 2Rx + x^2 = 0,$$

we can solve for x:

$$x = R \pm (R^2 - y^2)^{1/2}. \tag{5.44}$$

Let's just concern ourselves with values of x less than R, that is, we will study a hemisphere, open on the right, corresponding to the minus sign in Eq. (5.44). After expansion in a binomial series, x takes the form

$$x = \frac{y^2}{2R} + \frac{1y^4}{2^2 2! R^3} + \frac{1 \cdot 3y^6}{2^3 3! R^5} + \cdots. \tag{5.45}$$

This expression becomes quite meaningful as soon as we realize that the standard equation for a parabola with its vertex at the origin and its focus a distance f to the right [Fig. 5.48(b)] is simply

$$y^2 = 4fx. \tag{5.46}$$

Thus by comparing these two formulas, we see that if $4f = 2R$ (i.e., if $f = R/2$), the first contribution in the series can be thought of as parabolic, and the remaining

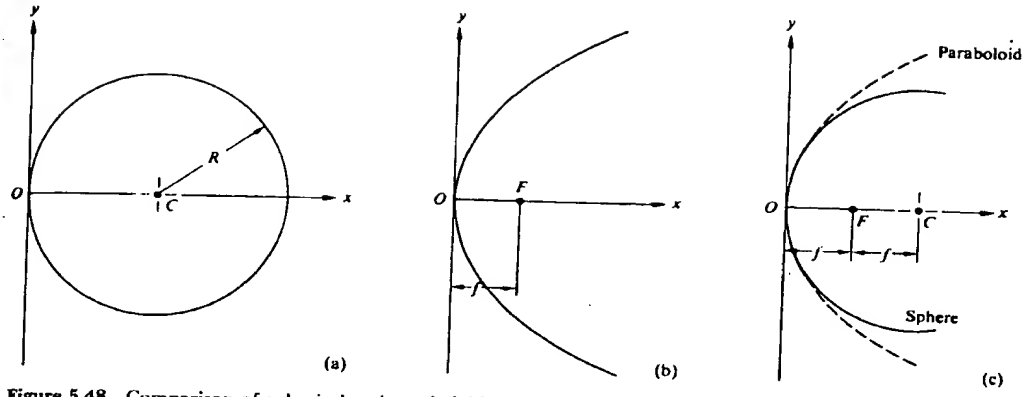

Figure 5.48 Comparison of spherical and paraboloidal mirrors.

terms represent the deviation. If that deviation is Δx, then

$$\Delta x = \frac{y^4}{8R^3} + \frac{y^6}{16R^5} + \cdots . \qquad (5.47)$$

Evidently this difference will be appreciable only when y is relatively large [Fig. 5.48(c)] in comparison to R. *In the paraxial region, that is, in the immediate vicinity of the optical axis, these two configurations will be essentially indistinguishable.* Thus if we talk about the paraxial theory of spherical mirrors as a first approximation, we can again embrace the conclusions drawn from our study of the stigmatic imagery of paraboloids. In actual use, however, y will not be so limited, and aberrations will appear. Moreover, aspherical surfaces produce perfect images only for pairs of axial points—they too will suffer aberrations.

ii) The Mirror Formula

The paraxial equation that relates conjugate object and image points to the physical parameters of a spherical mirror can be derived rather easily with the help of Fig. 5.49. To that end, observe that since $\theta_i = \theta_r$, the $\measuredangle SAP$ is bisected by $\overline{CA}$, which therefore divides the side $\overline{SP}$ of triangle SAP into segments proportional to the

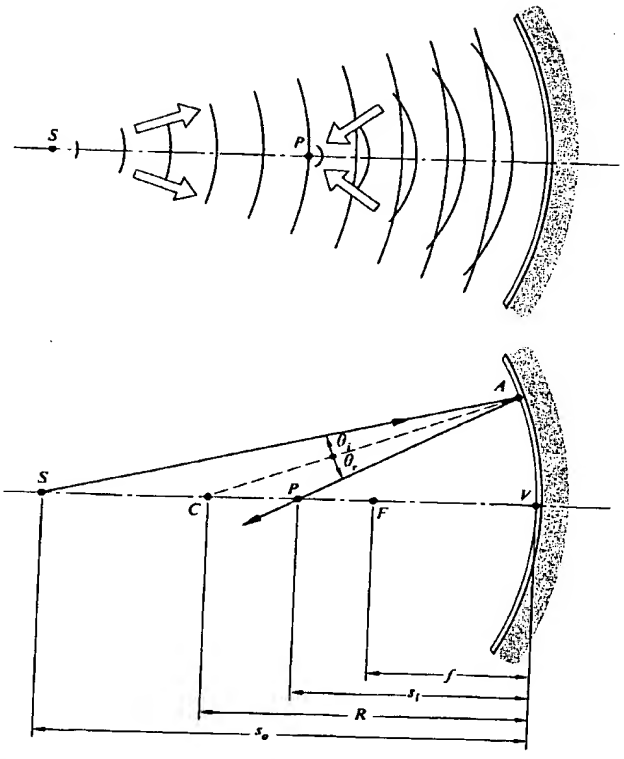

Figure 5.49 A concave spherical mirror.

remaining two sides, that is,

$$\frac{\overline{SC}}{\overline{SA}} = \frac{\overline{CP}}{\overline{PA}}. \tag{5.48}$$

Furthermore,

$$\overline{SC} = s_o - |R| \quad \text{and} \quad \overline{CP} = |R| - s_i,$$

where s_o and s_i are on the left and therefore positive. If we use the same sign convention for R as we did when we dealt with refraction, it will be negative here, because C is to the left of V (i.e., the surface is concave). Thus $|R| = -R$ and

$$\overline{SC} = s_o + R \quad \text{and} \quad \overline{CP} = -(s_i + R).$$

In the paraxial region $\overline{SA} \approx s_o$, $\overline{PA} \approx s_i$, and so Eq. (5.48) becomes

$$\frac{s_o + R}{s_o} = -\frac{s_i + R}{s_i}$$

or

$$\frac{1}{s_o} + \frac{1}{s_i} = -\frac{2}{R}, \tag{5.49}$$

which is often referred to as the **mirror formula**. It is equally applicable to concave ($R < 0$) and convex ($R > 0$) mirrors. The primary or object focus is again defined

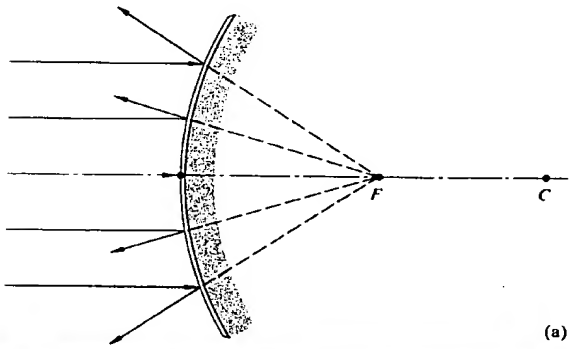

(a)

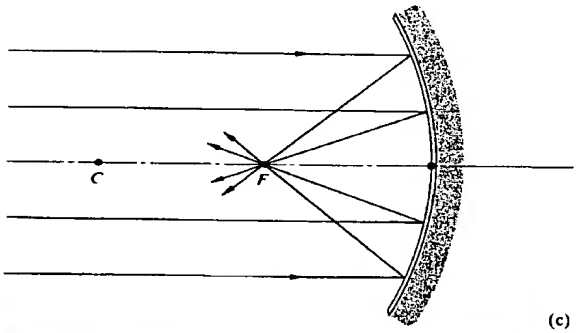

(c)

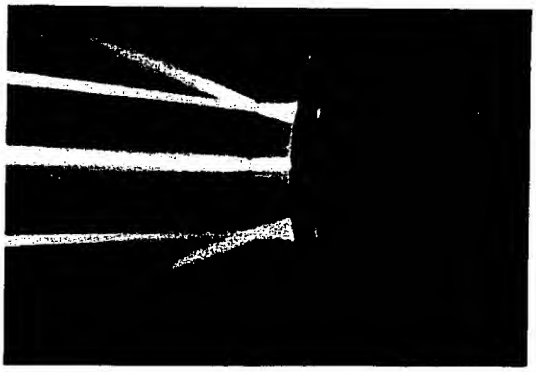

Figure 5.50 Focusing of rays via a spherical mirror. (Photos by E.H.)

by

$$\lim_{s_i \to \infty} s_o = f_o,$$

and the secondary or image focus corresponds to

$$\lim_{s_o \to \infty} s_i = f_i.$$

Consequently, from Eq. (5.49)

$$\frac{1}{f_o} + \frac{1}{\infty} = \frac{1}{\infty} + \frac{1}{f_i} = -\frac{2}{R},$$

to wit, $f_o = f_i = -R/2$, as we know from Fig. 5.45(c). Thus, dropping the subscripts on the focal lengths, we have

$$\frac{1}{s_o} + \frac{1}{s_i} = \frac{1}{f}. \qquad (5.50)$$

Observe that f will be positive for concave mirrors ($R < 0$) and negative for convex mirrors ($R > 0$). In the latter instance the image is formed behind the mirror and is virtual (Fig. 5.50).

iii) Finite Imagery

The remaining mirror properties are so similar to those of lenses and spherical refracting surfaces that we need only mention them briefly, without repeating the entire logical development of each item. Within the restrictions of paraxial theory, any parallel off-axis bundle of rays will be focused to a point on the *focal plane* passing through F normal to the optical axis. Likewise, a finite planar object perpendicular to the optical axis will be imaged (to a first approximation) in a plane similarly oriented. Essentially we are saying that each object point will have a corresponding image point in the plane. This is certainly true for a plane mirror, but it only approximates the case for other configurations. To be sure, if a spherical mirror is appropriately restricted in its operation, the reflected waves arising from each permitted object point will closely approximate spherical waves. Under such circumstances good finite images of extended objects can be formed (Fig. 5.51). Just as each image point produced by a thin lens lies along a straight line through the optical center O, each

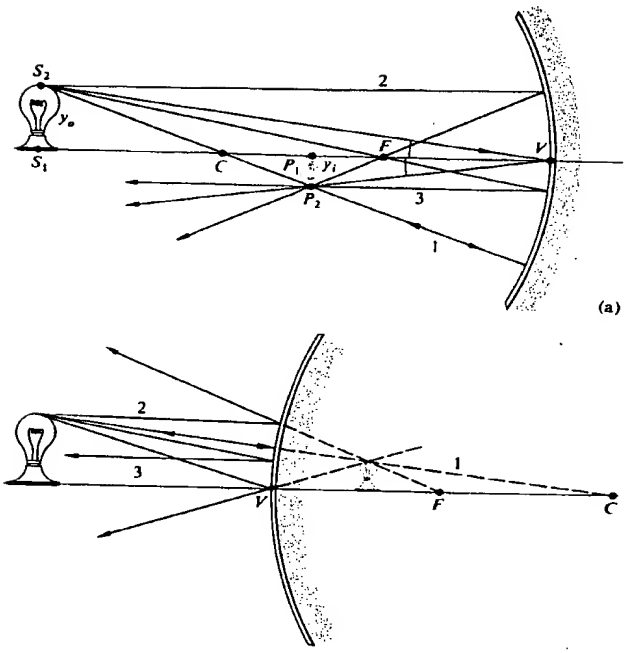

Figure 5.51 Finite imagery with spherical mirrors.

image point for a spherical mirror will lie on a ray passing through both the center of curvature C and the object point. As with the thin lens (Fig. 5.24), the graphic location of the image is quite straightforward. Once more the top of the image is located at the intersection of two rays, one initially parallel to the axis and passing through F after reflection, and the other going straight through C (Fig. 5.52). The ray from any off-axis object point to the vertex forms equal angles with the optical axis on reflection and is therefore particularly convenient to construct as well. So too is the ray that first passes through the focus and after reflection emerges parallel to the axis.

Notice that triangles S_1S_2V and P_1P_2V in Fig. 5.51(a) are similar, and hence their sides are proportional. Taking y_i to be negative, as we did before, since it is below the axis, we find that $y_i/y_o = -s_i/s_o$, which of

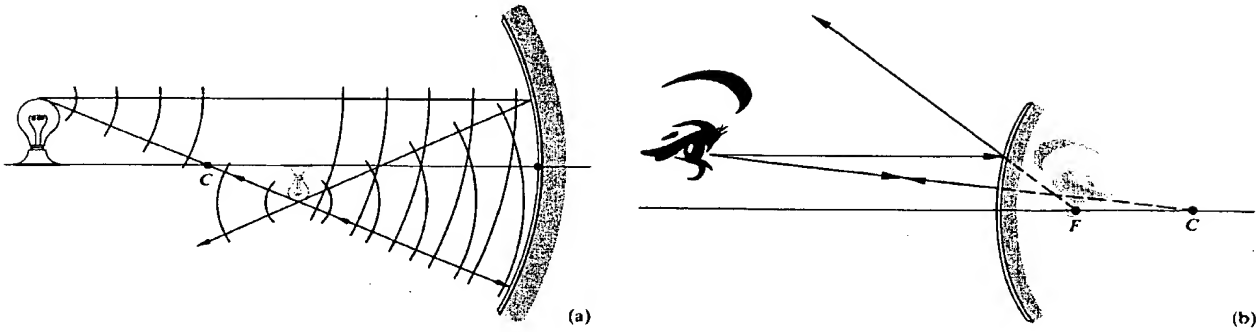

Figure 5.52 (a) Reflection from a concave mirror. (b) Reflection from a convex mirror.

course is equal to M_T, the *transverse magnification*, identical to that of the lens (5.25).

The only equation that contains information about the structure of the optical element (n, R, etc.) is that for f, and so, rather understandably, it differs for the thin lens and spherical mirror. The other functional expressions that relate s_o, s_i, and f or y_o, y_i, and M_T are, however, precisely the same. The only alteration in the previous sign convention appears in Table 5.4, where s_i on the left of V is now taken as positive. The striking similarity between the properties of a concave mirror and a convex lens on one hand and a convex mirror and a concave lens on the other are quite evident from a comparison of Tables 5.3 and 5.5, which are identical in all respects.

The properties summarized in Table 5.5 and depicted pictorially in Fig. 5.53 can easily be verified empirically. If you don't have a spherical mirror at hand, a fairly crude but functional one can be made by carefully shaping aluminum foil over a spherical form, such as the end of a light bulb (in that particular case R and therefore f will be small). A rather nice qualitative experiment involves examining the image of some small object formed by a short focal-length concave mirror. As you move it toward the mirror from beyond a distance of $2f = R$, the image will gradually increase, until at $s_o = 2f$ it will appear inverted and life-size. Bringing it closer will cause the image to increase even more, until it fills the entire mirror with an unrecognizable blur. As s_o becomes smaller, the now erect, magnified image will continue to decrease until the object finally rests on the mirror, where the image is again life-size.

Table 5.4 Sign convention for spherical mirrors.

Quantity	Sign	
	+	−
s_o	Left of V, real object	Right of V, virtual object
s_i	Left of V, real image	Right of V, virtual image
f	Concave mirror	Convex mirror
R	C right of V, convex	C left of V, concave
y_o	Above axis, erect object	Below axis, inverted object
y_i	Above axis, erect image	Below axis, inverted image

Table 5.5 Images of real objects formed by spherical mirrors.

Concave				
Object	Image			
Location	Type	Location	Orientation	Relative size
$\infty > s_o > 2f$	Real	$f < s_i < 2f$	Inverted	Minified
$s_o = 2f$	Real	$s_i = 2f$	Inverted	Same size
$f < s_o < 2f$	Real	$\infty > s_i > 2f$	Inverted	Magnified
$s_o = f$		$\pm\infty$		
$s_o < f$	Virtual	$\lvert s_i\rvert > s_o$	Erect	Magnified
Convex				
Object	Image			
Location	Type	Location	Orientation	Relative size
Anywhere	Virtual	$\lvert s_i\rvert < \lvert f\rvert$, $s_o > \lvert s_i\rvert$	Erect	Minified

If you are not moved by all of this to jump up and make a mirror, you might try examining the image formed by a shiny spoon—either side will be interesting.

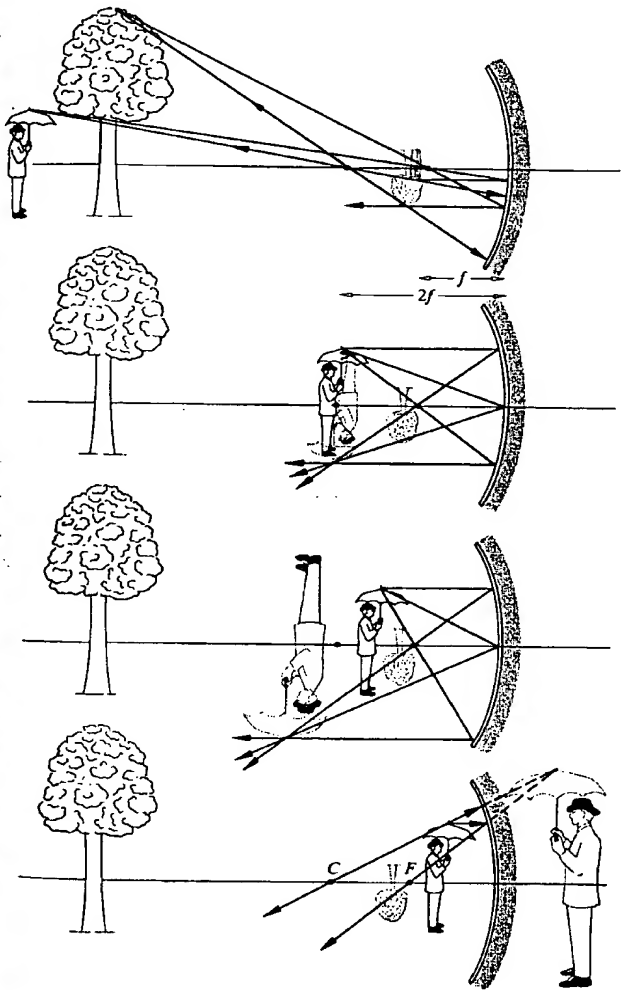

Figure 5.53 The image-forming behavior of a concave spherical mirror.

5.5 PRISMS

Prisms have many different roles in optics; there are prism combinations that serve as beam-splitters (see Section 4.3.4), polarizing devices (see Section 8.4.3), and even interferometers. Despite this diversity, the vast majority of applications make use of only one of two main prism functions. First, a prism can serve as a dispersive device, as it does in a variety of spectrum analyzers. That is to say, it is capable of separating, to some extent, the constituent frequency components in a polychromatic light beam. You might recall that the term *dispersion* was introduced earlier (Section 3.5.1) in connection with the frequency dependence of the index of refraction, $n(\omega)$, for dielectrics. In fact, the prism provides a highly useful means of measuring $n(\omega)$ over a broad range of frequencies and for a wide variety of materials (including gases and liquids). Its second and more common function is to effect a change in the orientation of an image or in the direction of propagation of a beam. Prisms are incorporated in many optical instruments, often simply to fold the system into a confined space. There are inversion prisms, reversion prisms, and prisms that deviate a beam without inversion or reversion—and all of this without dispersion.

5.5.1 Dispersing Prisms

Nowadays prisms come in a great variety of sizes and shapes and perform an equally great variety of functions (Fig. 5.54). Let's first consider the group known as **dispersing prisms**. Typically, a ray entering a dispersing prism, as in Fig. 5.55, will emerge having been deflected from its original direction by an angle δ known as the *angular deviation*. At the first refraction the ray is deviated through an angle $(\theta_{i1} - \theta_{t1})$, and at the second refraction it is further deflected through $(\theta_{i2} - \theta_{i2})$. The total deviation is then

$$\delta = (\theta_{i1} - \theta_{t1}) + (\theta_{i2} - \theta_{i2}).$$

Since the polygon $ABCD$ contains two right angles, $\measuredangle BCD$ must be the supplement of the *apex angle* α. As the exterior angle to triangle BCD, α is also the sum

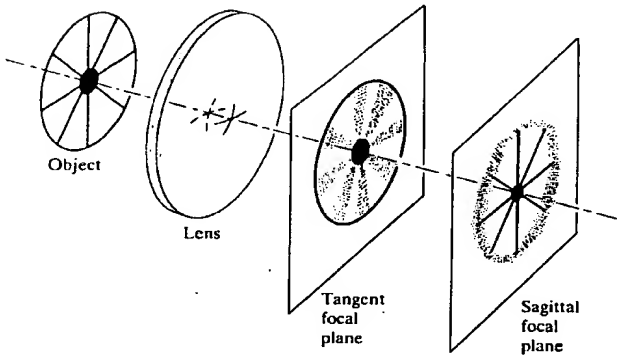

Figure 6.24 Images in the tangent and sagittal focal planes.

The existence of the sagittal and tangential foci can be verified directly with a fairly simple arrangement. Place a positive lens with a short focal length (about 10 or 20 mm) in the beam of a He–Ne laser. Position another positive test lens with a somewhat longer focal length far enough away so that the now diverging beam fills that lens. A convenient object, to be located between the two lenses, is a piece of ordinary wire screening (or a transparency). Align it so the wires are horizontal (x) and vertical (y). If the test lens is rotated roughly 45° about the vertical (with the x-, y-, and z-axes fixed in the lens), astigmatism should be observable. The meridional is the xz-plane (z being the lens axis, now at about 45° to the laser axis), and the sagittal plane corresponds to the plane of y and the laser axis. As the wire mesh is moved toward the test lens, a point will be reached where the horizontal wires are in focus on a screen beyond the lens, whereas the vertical wires are not. This is the location of the sagittal focus. Each point on the object is imaged as a short line in the meridional (horizontal) plane, which accounts for the fact that only the horizontal wires are in focus. Moving the mesh slightly closer to the lens will bring the vertical lines into clarity while the horizontal ones are blurred. This is the tangential focus. Try rotating the mesh about the central laser axis while at either focus.

Note that unlike visual astigmatism, which arose from an actual asymmetry in the surfaces of the optical system, the third-order aberration by that same name applies to spherically symmetrical lenses.

Mirrors, with the singular exception of the plane mirror, suffer much the same monochromatic aberrations as do lenses. Thus although a paraboloidal mirror is free of SA for an infinitely distant axial object point, its off-axis imagery is quite poor due to astigmatism and coma. This strongly restricts its use to narrow field devices, such as searchlights and astronomical telescopes. A concave spherical mirror shows SA, coma, and astigmatism. Indeed one could draw a diagram just like Fig. 6.23 with the lens replaced by an obliquely illuminated spherical mirror. Incidentally, such a mirror displays appreciably less SA than would a simple convex lens of the same focal length.

iv) Field Curvature

Suppose we had an optical system that was free of all the aberrations thus far considered. There would then be a one-to-one correspondence between points on the object and image surfaces (i.e., stigmatic imagery). We mentioned earlier (Section 5.2.3) that a planar object normal to the axis will be imaged approximately as a plane only in the paraxial region. At finite apertures the resulting curved stigmatic image surface is a manifestation of the primary aberration known as **Petzval field curvature**, after the Hungarian

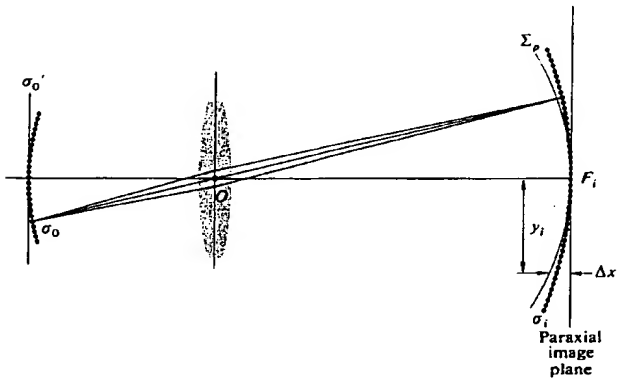

Figure 6.25 Field curvature.

mathematician Josef Max Petzval (1807–1891). The effect can readily be appreciated by examining Figs. 5.22 (p. 141) and 6.25. A spherical object segment σ_o is imaged by the lens as a spherical segment σ_i, both centered at O. Flattening out σ_o into the plane σ_o' will cause each object point to move toward the lens along the concomitant chief ray, thus forming a paraboloidal *Petzval surface* Σ_P. Whereas the Petzval surface for a positive lens curves *inward* toward the object plane, for a negative lens it curves *outward*, that is, away from that plane. Evidently, a suitable combination of positive and negative lenses will negate field curvature. Indeed, the displacement Δx of an image point at height y_i on the Petzval surface from the paraxial image plane is given by

$$\Delta x = \frac{y_i^2}{2} \sum_{j=1}^{m} \frac{1}{n_j f_j}, \tag{6.43}$$

where n_j and f_j are the indices and focal lengths of the m thin lenses forming the system. This implies that the Petzval surface will be unaltered by changes in the positions or shapes of the lenses or in the location of the stop, so long as the values of n_j and f_j are fixed. Notice that for the simple case of two thin lenses ($m = 2$) having any spacing, Δx *can be made zero* provided that

$$\frac{1}{n_1 f_1} + \frac{1}{n_2 f_2} = 0$$

or, equivalently,

$$n_1 f_1 + n_2 f_2 = 0. \tag{6.44}$$

This is the so-called *Petzval condition*. As an example of its use, suppose we combine two thin lenses, one positive, the other negative, such that $f_1 = -f_2$ and $n_1 = n_2$. Since

$$\frac{1}{f} = \frac{1}{f_1} + \frac{1}{f_2} - \frac{d}{f_1 f_2}, \tag{6.8}$$

$$f = \frac{f_1^2}{d},$$

the system can satisfy the Petzval condition, have a flat field, and still have a finite positive focal length.

In visual instruments a certain amount of curvature can be tolerated, because the eye can accommodate for it. Clearly, in photographic lenses field curvature is most undesirable, since it has the effect of rapidly blurring the off-axis image when the film plane is at F_i. An effective means of nullifying the inward curvature of a positive lens is to place a negative *field flattener* lens near the focal plane. This is often done in projection and photographic objectives when it is not otherwise practicable to meet the Petzval condition (Fig. 6.26). In this position the flattener will have little effect on other aberrations (take another look at Fig. 6.7).

Astigmatism is intimately related to field curvature. In the presence of the former aberration, there will be *two* paraboloidal image surfaces, the tangential, Σ_T, and the sagittal, Σ_S (as in Fig. 6.27). These are the loci of all the primary and secondary images, respectively, as the object point roams over the object plane. At a given height (y_i), a point on Σ_T always lies three times as far from Σ_P as does the corresponding point on Σ_S, and both are on the same side of the Petzval surface (Fig. 6.27). When there is no astigmatism Σ_S and Σ_T coalesce on Σ_P. It is possible to alter the shapes of Σ_S and Σ_T by bending or relocating the lenses or by moving the stop. The configuration of Fig. 6.27(b) is known as an *artificially flattened* field. A stop in front of an inexpensive meniscus box camera lens is usually arranged to produce just this effect. The surface of least confusion, Σ_{LC}, is

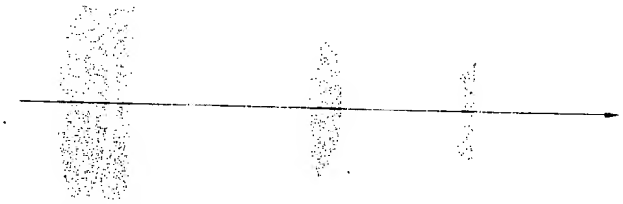

(a) Petzval lens with field flattener

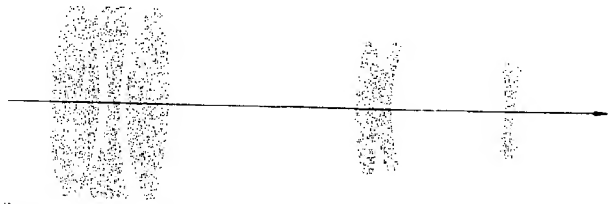

(b) 16 mm projection lens

Figure 6.26 The field flattener.

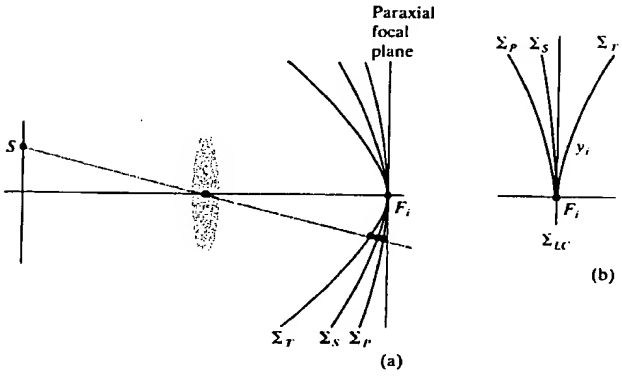

Figure 6.27 The tangential, sagittal and Petzval image surfaces.

planar, and the image there is tolerable, losing definition at the margins because of the astigmatism. That is to say, although their loci form Σ_{LC}, the circles of least confusion increase in diameter with distance off the axis. Modern good-quality photographic objectives are generally *anastigmats*; that is, they are designed so that Σ_S and Σ_T cross each other, yielding an additional off-axis angle of zero astigmatism. The Cooke Triplet, Tessar, Orthometer, and Biotar (Fig. 5.112) are all anastigmats, as is the relatively fast Zeiss Sonnar, whose residual astigmatism is illustrated graphically in Fig. 6.28. Note the relatively flat field and small amount of astigmatism over most of the film plane.

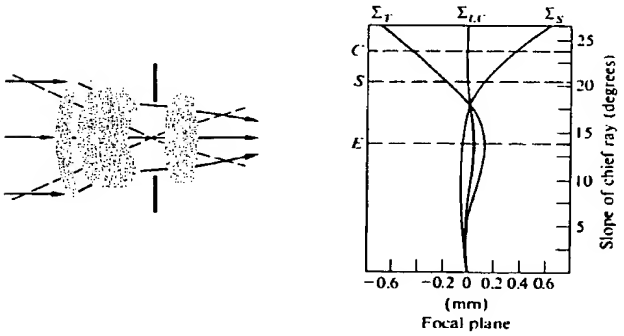

Figure 6.28 A typical Sonnar. The markings *C*, *S*, and *E* denote the limits of the 35-mm film formate (field stop), i.e., corners, sides, and edges. The Sonnar family lies between the double Gauss and the triplet.

Let's return briefly to the Schmidt camera shown in Fig. 5.107 (p. 198), since we are now in a better position to appreciate how it functions. With a stop at the center of curvature of the spherical mirror, all chief rays, which by definition pass through *C*, are incident normally on the mirror. Moreover, each pencil of rays from a distant object point is symmetrical about its chief ray. In effect, each chief ray serves as an optical axis, so there are no off-axis points and, in principle, no coma or astigmatism. Instead of attempting to flatten the image surface, the designer has coped with curvature by simply shaping the film plate to conform with it.

v) Distortion

The last of the five primary, monochromatic aberrations is **distortion**. Its origin lies in the fact that the transverse magnification, M_T, may be a function of the off-axis image distance, y_i. Thus, that distance may differ from the one predicted by paraxial theory in which M_T is constant. In other words, distortion arises because different areas of the lens have different focal lengths and different magnifications. In the absence of any of the other aberrations, distortion is manifest in a misshaping of the image as a whole, even though each point is sharply focused. Consequently, when processed by an optical system suffering *positive* or *pincushion distortion*, a square array deforms, as in Fig. 6.29(b). In that instance, each image point is displaced radially outward from the center, with the most distant points moving the greatest amount (i.e., M_T increases with y_i). Similarly, *negative* or *barrel distortion* corresponds to the situation in which M_T decreases with the axial distance, and in effect, each point on the image moves radially inward toward the center [Fig. 6.29(c)]. Distortion can easily be seen by just looking through an aberrant lens at a piece of lined or graph paper. Fairly thin lenses will show essentially no distortion, whereas ordinary positive or negative, thick, simple lenses will generally suffer positive or negative distortion, respectively. The introduction of a stop into a system of thin lenses is